Catalysis Today 423 (2023) 114014

Contents lists available at ScienceDirect

Catalysis Today

journal homepage: www.elsevier.com/locate/cattod

Towards selective synthesis of quinoxalines by using transition metals-doped carbon aerogels

Marina Godino-Ojer [a], Sergio Morales-Torres [b], Francisco J. Maldonado-Hódar [b,*], Elena Pérez-Mayoral [c,*]

[a] Facultad de Ciencias Experimentales, Universidad Francisco de Vitoria, UFV, Ctra. Pozuelo-Majadahonda km 1.800, Pozuelo de Alarcón, 28223 Madrid, Spain
[b] NanoTech – Nanomateriales y Tecnologías Químicas Sostenibles, Departamento de Química Inorgánica, Facultad de Ciencias, Universidad de Granada, Avenida de Fuente Nueva, 18071 Granada, Spain
[c] Departamento de Química Inorgánica y Química Técnica, Universidad Nacional de Educación a Distancia, UNED, Urbanización Monte Rozas, Avenida Esparta s/n, Ctra de Las Rozas al Escorial Km 5, 28232 Las Rozas-Madrid, Spain

ARTICLE INFO

Keywords:
Transition metals
Carbon aerogels
Heterogeneous catalysis
Fine chemicals

ABSTRACT

Transition metal (TM)-carbon aerogels, where TM = Mo, Fe, Co or Cu, were found to be active and selective catalysts for the synthesis of quinoxalines **1**, from *o*-phenylenediamine **2** and α-hydroxy ketones **3**, becoming an efficient and sustainable alternative to other carbon-based catalysts or even MOF.

Doping metal phase consisting of the corresponding metal oxides but also as zero-valent metals depending on the metal and carbonization temperature, and metal loading at the surface of carbon aerogel are key factors conditioning both reactivity and selectivity. Although metal oxides are probably the predominant active catalytic species, zero-valent metals nanoparticles (Cu^0 or Co^0) could be implied in the last dehydrogenation step of the reaction. Moreover, the additional functionalization with oxygenated surface groups (Co-1000PO catalyst) resulted on an enhanced reactivity probably due to the cooperation between both functions. Remarkably, Mo-500 catalyst was the most efficient sample selectively leading to the quinoxaline **1a** in high conversion.

Finally, our results strongly suggest different operative pathways when using TM-doped carbon aerogels depending on the metallic phase at the carbon surface. While TM-doped carbon aerogels (where TM = Fe, Co, or Cu) probably act catalyzing a sequential acid-base steps and subsequent aromatization leading to the corresponding quinoxaline **1a**, Mo-doped catalyst would work *via* the initial oxidation of α-hydroxy ketones followed by condensation-dehydration reactions.

1. Introduction

Nanostructured carbon gels are materials of great interest with application in catalysis [1]. In the last years, carbon gels have been also reported for environmental applications such as treatments of air and water effluents [2], clean energy production, transformation or storage of energy, or green and sustainable chemistry [3]. Because they are synthesized by strictly controlled procedures using pure reactants, also exhibit high, tuneable porosity and good mechanical properties. In the case of metal-doped carbon gels, the metal precursor used for the synthesis greatly influences the final characteristics of the material, since the metal is involved in all the synthesis steps – polymerization, carbonization and/or activation – [4]. During the carbonization process the formation of different metallic species – oxides, zero valent metals, metallic carbides – depending on the nature of the precursor and the experimental conditions of synthesis is produced. It is noteworthy that the absence of ashes in this type of materials is an important issue because it guarantees that the dopant metal is responsible of catalytic performance without interferences.

Recently, we applied carbon aerogels as promising candidates for the synthesis of nitrogen-containing heterocyclic systems, *via* the Friedländer reaction [5], as the simplest synthetic approach to produce quinolines and related compounds. Interestingly, a recent study involving metal-free carbon aerogels confirmed that relatively strong π – π stacking interactions between carbon support and reagents take place, indicating the involvement of the carbon matrix in the reaction. In addition, the porosity and carboxylic acid groups (–CO_2H) at the carbon surface are behind the enhanced catalytic performance [6]. Metal-doped

* Corresponding authors.
E-mail addresses: fjmaldon@ugr.es (F.J. Maldonado-Hódar), eperez@ccia.uned.es (E. Pérez-Mayoral).

https://doi.org/10.1016/j.cattod.2023.01.021
Received 28 October 2022; Received in revised form 16 January 2023; Accepted 24 January 2023
Available online 25 January 2023

carbon gels have been also reported in other fine chemical syntheses, such as citral selective hydrogenation [7], Michael addition reactions [8] and quinoline synthesis catalyzed by Co^0 and Cu^0-doped aerogels [9, 10] but also CoO or ZnO supported on carbon aerogels [11,12]; relationships between properties of the materials – active phase nature and dispersion, textural properties and surface chemistry – and catalytic performance were reported.

Considering the high potential of carbon aerogels for the synthesis of heterocyclic systems, we report herein different carbon aerogels doped with transition metals (TMs) – Mo, Fe, Co or Cu – , active and selective in the synthesis of quinoxalines **1**, from *o*-phenylendiamine **2** and different α-hydroxy ketones **3** (Scheme 1).

Quinoxalines are nitrogen heterocycles considered as privileged structural scaffolds commonly found in natural products and pharmaceuticals. TMs have been extensively investigated for quinoxaline catalytic syntheses, especially the first-row ones due to the greater abundance, low toxicity, low cost, among other advantages [13]. In this context, structurally different heterogeneous catalysts have been reported for this synthesis such as manganese oxide octahedral molecular sieves (OMS-2) [14], iron exchanged 12-molybdophosphoric acid (FeMPA) [15], $CuCl_2$ combined with molecular sieve 4A [16], Amberlite IR-120 H [17] and even metal organic-frameworks (MOFs) – synthetic Cu(BDC) more active than zeolites [18] or commercial available Basolites [19] –.

TM carbon-based catalysts have been also reported for this synthesis such as ruthenium immobilized on charcoal [20], sophisticated gold–carbon nanotube nanohybrid [21] and nitrogen-doped carbons supported cobalt-based nanocatalysts [22], both in the presence of bases as additives, but also Co-based catalyst supported on N,P co-doped porous carbon [23].

Accepted reaction mechanisms for the synthesis of quinoxalines from diamines and α-hydroxy ketones comprise either sequential acid catalyzed reactions and final aromatization [22] or alcohol dehydrogenations followed by double condensation [15]. However, only a few papers include mechanistic information concerning this synthesis (*see* Results and Discussion section). At this regard, we recently reported on a new sustainable alternative by using acidic porous carbon catalysts derived from vegetal biomass efficient for the aerobic one-pot synthesis of quinoxalines, from both different 1,2-diamines and α-hydroxy ketones, in absence of any additive [24]. Our experimental and theoretical results demonstrated that the reaction is mainly controlled by a combination of acid strength of oxygen-containing functions and porosity. Particularly, the reaction can be catalyzed by $-CO_2H$ functions following the sequence: i) nucleophilic addition between reactants and subsequent dehydration, ii) successive imine-enamine and keto-enol tautomerisms, iii) heterocyclization followed by dehydration, and finally (iv) aromatization to give nitrogenated heterocycles. Based on that, when using the carbon aerogels doped with TMs of our choice it would be expected a synergic effect between TMs and carbon and chemical surface in the quinoxaline synthesis.

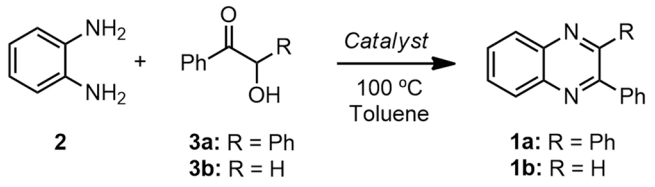

2 **3a:** R = Ph **3b:** R = H **1a:** R = Ph **1b:** R = H

Scheme 1. Synthesis of quinoxaline **1** from *o*-phenylendiamine **2** and α-hydroxy ketones **3**, in toluene, at 100 °C, catalyzed by carbon aerogels.

2. Materials and methods

2.1. Synthesis of catalysts

Carbon aerogels doped with TMs were prepared following the method described by Maldonado-Hódar et al. [1]. Briefly, the organic fraction is prepared from resorcinol (R) and formaldehyde (F) mixtures (molar R/F = ½) in aqueous solutions. Ammonium heptamolybdate or iron, cobalt or copper acetates were used as precursors of Mo, Fe, Co or Cu-doped materials, respectively, dissolved in the previous solution. The amount of metal-salt precursors were fitted in each case to obtain a metal concentration of 1 wt% on the total solution, although in the case of Cu-doped aerogels a 3 wt% sample was also prepared. After obtaining a homogeneous solution by stirring, the TM-RF solutions were cast into glass molds, polymerized and cured (30 °C /1 day, 50 °C /2 days and 80 °C /5 days) and then dried with supercritical CO_2. Carbon aerogels were obtained by pyrolysis of the organic aerogels by heating up to 500 or 1000 °C in N_2 flow, with a heating rate of 1.5 °C min^{-1}. The carbon aerogels will be referred in the text by adding the carbonization temperature to the metal-doping (indicating Cu3 in the case of high Cu-loading).

2.2. Characterization of the catalysts

The textural characteristics of the samples were determined by combination of N_2 physical adsorption at – 196 °C (Quadrasorb SI, Quantachrome) and mercury porosimetry (Quantachrome Autoscan60). The BET equation was applied to the N_2 adsorption for determining BET surface areas (S_{BET}). From mercury intrusion curves, the particle density (ρ_p), the pore size distribution (PSD), the mesopore volume (V_2), (mesopores with a diameter of between 3.7 and 50 nm) and macropore volume (V_3), for pores with a diameter larger than 50 nm, were determined.

The total metal loading was analysed by thermogravimetric analysis (TG) and compared with the surface metal loading determined by X-ray photoelectron spectroscopy, XPS (Physical Electronics Versa Probe II PHI, Chanhassen, MN, USA). Survey and multi-region spectra were recorded at the C1s, O1s, and M (Fe, Co, Cu) 2p and Mo 3d photoelectron peaks. The morphology of the prepared materials was analyzed by SEM (LEO, Carl Zeiss, GEMINI-1430VP). X-ray diffraction (XRD) patterns were obtained using a Bruker D8 Advance diffractometer (Cu Kα radiation at $\lambda = 1.5406$ Å) to determine the nature of surface metal particles. Assignation of phases according to the ICDD (International Centre for Diffraction Data) cards. The metal size and particle size dispersion were obtained from the scanning transmission electron microscopy (STEM) images, using an FEI Titan G2 60–300 microscope equipped with energy-dispersive X-ray spectroscopy (EDX) microanalysis and mapping systems.

2.3. Catalytic performance

A mixture of *o*-phenylendiamine **2** (1 mmol) and the corresponding α-hydroxy ketone **3** (1 mmol), in toluene (5 mL), in a three-necked vessel, equipped with reflux condenser, thermometer and septum, was placed on a multiexperiment work station StarFish (Radleý's Discovery Technologies IUK). When the temperature reaches 100 °C, the catalyst (50 mg) was added, and the reaction mixture was stirred during 240 min. The samples were periodically taken at 60, 120, 180 and 240 min, the catalyst filtered off and the solvent evaporated under vacuum. In order to avoid mass transfer limitations, catalysts were milled and sieved to a particle size (dp) < 0.25 mm. Before use, carbon catalysts were activated at 60 °C overnight.

The reactions were qualitatively followed by TLC chromatography performed on DC-Aulofolien/Kieselgel 60 F245 (Merk) using mixtures of CH_2Cl_2/EtOH 98:2 as eluent.

The reaction products were characterized by ^{1}H NMR spectroscopy.

NMR spectra were recorded by using a Bruker AVIII spectrometer (400 MHz for ^{1} H). ^{1}H chemical shifts are referenced to internal tetramethylsilane. Characterization data of synthetized benzodiazepines **1** are in good agreement with those previously reported using other catalytic systems [25].

Conversion is defined as the fraction of reactant **2** transformed at each reaction time into compounds determined by ^{1}H NMR. Selectivity of the process is based on the amount of the desired products ($S = C/C_{Total}$ where S and C are selectivity and conversion values to the corresponding product, respectively, and C_{Total} is the total conversion of reactant **2**).

3. Results and discussion

3.1. Synthesis and characterization of the catalysts

These materials present differences on porosity and oxidation states of metallic phases depending on the used metal precursor and carbonization temperature. The weight loss (WL) observed during carbonization, the total metal loading obtained by burning a fraction of the carbonized samples and textural characteristics of carbon aerogels are summarized in Table 1. As observed (Table 1), all the samples present after carbonization at 500 ºC a similar pyrolysis degree. This parameter also increased when increasing the carbonization temperature from 500° to 1000°C (as showed for the case of Co-doped carbon aerogels). The carbonization processes were also simulated by TG (Fig. S1) denoting that the WL associated to the carbonization occurs in three main steps (bellow 200–250 ºC desorption of solvents and unreacted precursors, between 250 and 400 and 400 – 600, breaking and reorganization of C-O and C-C bonds, respectively). The TG/DTG profiles depend on the metal present and no significant WL occurs from 700 to 800 ºC [26].

Moreover, this process leads to a deep restructuration of the porosity. Co-500 is a mesoporous sample, with a large mesopore volume (V_2) of homogeneous pores with a mean diameter at around 17 nm (Fig. 1), whereas after increasing the carbonization temperature until 1000 °C, Co-1000 became a macroporous sample (V_3 increased at the expense of V_2), with a mean pore diameter of 50 nm (Table 1 and Fig. 1). This fact leads to a significant reduction of BET surface area values, because macropores present a low surface regarding mesopores. The rest of samples are also macroporous catalysts, with high volumes of large macropores (Fig. 1). In all cases, the open porosity (meso + macropores) is around 1.4 $cm^3\ g^{-1}$ leading also to a very similar bulk density (ρ_p) values. In the case of Cu-doped catalysts, when metal loading increase from 1% to 3%, it does not significantly modify the pore size distribution of samples carbonized at 1000 ºC (Fig. S2), although there is a microporosity decrease which leads also to a decrease of the SBET surface area from 850 to 740 m^2g^{-1}.

In carbon aerogels, the macro-mesoporous structure is formed as consequence of the 3D-stacking of primary particles, increasing therefore the pore size with increasing the particle size. This fact was also confirmed by SEM images (Fig. 2) where the coral like structure characteristic of carbon gels is observed. The different particle size is due also to the distinct catalytic effect of the metal present on the R-F polymerization mixture – carbonization processes [27] –because all the other parameters – concentration of monomers, polymerization temperature/time, drying/carbonization procedure, etc – were maintained. Together the commented porosity changes, the carbonization temperature also determines the nature and dispersion of the metal phase. At this regard, when increasing this parameter, evidently also increased the degree of reduction of metal phases by the carbon support favouring simultaneously the metal particle size (sintering).

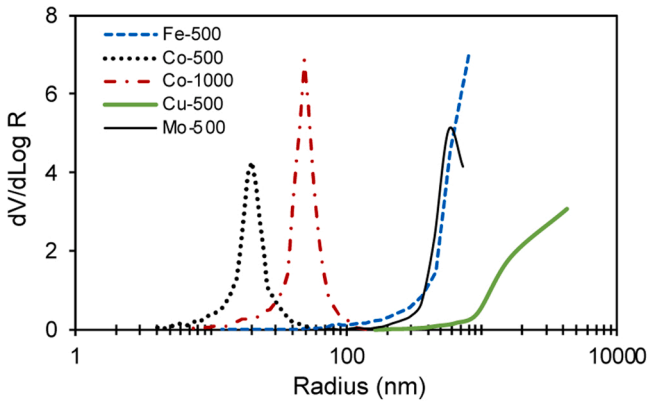

Fig. 1. Pore size distribution (PSD) of the different TM-doped carbon aerogels obtained by mercury porosimetry.

XRD patterns depicted in Fig. 3 showed that most of the catalysts when carbonized at 500 °C remain practically amorphous; no peaks associated to the metallic phase were found (except in the case of Fe-500 catalysts) and only the large bands at around 25 and 44° denote an incipient carbon ordering. At this temperature, the only crystalline particles detected correspond to hematite phase (Fe_2O_3, peaks at 2θ = 35.6, 57.1, and 62.7°) in sample Fe-500. This metallic nanostructure clearly was observed by TEM (Fig. 4a). Nevertheless, after carbonization at 1000 °C, metal oxides are progressively reduced by the carbon phase. In the case of Co-1000, metal appears totally reduced to Co^0 (peaks at 44, 51 and 75°) together a marked peak at 26° associated to the (002) diffraction of graphitic microcrystals. These facts were also pointed out by TEM images (Fig. 4d), where the formation of round shaped graphitic structures, some of them formed surrounding the metal nanoparticles, were observed. Thus, while metal nanoparticles are reduced and sintered, the carbon phase becomes progressively more structured, forming also graphitic structures depending on the metal present. At low temperatures, metals are very well dispersed (Fig. 4b and c), mainly in the metal oxide forms, on amorphous carbon and highly porous phases; metal size, metal reduction degree and graphitization of the carbon phase progressively were favoured by carbonization temperature.

The chemical surface nature of the catalysts was also analysed by XPS (Table 2 and Fig. S3). The assignation of the XPS components were carried out according to the bibliographic references [27–29). In general (no fitting is shown), the C1s peak denoted four different types of carbon bonds with increasing Binding Energy (BE): C=C bonds of aromatic sp^2 structures (~284.9 eV), C–O and hydroxyl groups (~286.0 eV), C=O

Table 1
Textural characterization of metal-doped carbon aerogels.

Sample	Weight loss (%)	Metal (%)	ρ_p (g cm^{-3})	S_{BET} ($m^2\ g^{-1}$)	V_3 ($cm^3\ g^{-1}$)	V_2 ($cm^3\ g^{-1}$)
Fe-500	43	3.3	0.44	482	1.516	0.000
Co-500	48	4.2	0.50	660	0.122	0.887
Co-1000	55	4.5	0.54	388	0.995	0.092
Cu-500	49	3.4	0.47	286	1.440	0.000
Mo-500	45	3.9	0.50	481	1.399	0.000

ρ_p: Particle density; S_{BET}: BET surface area; V_2: mesopore volume and V_3: macropore volume.

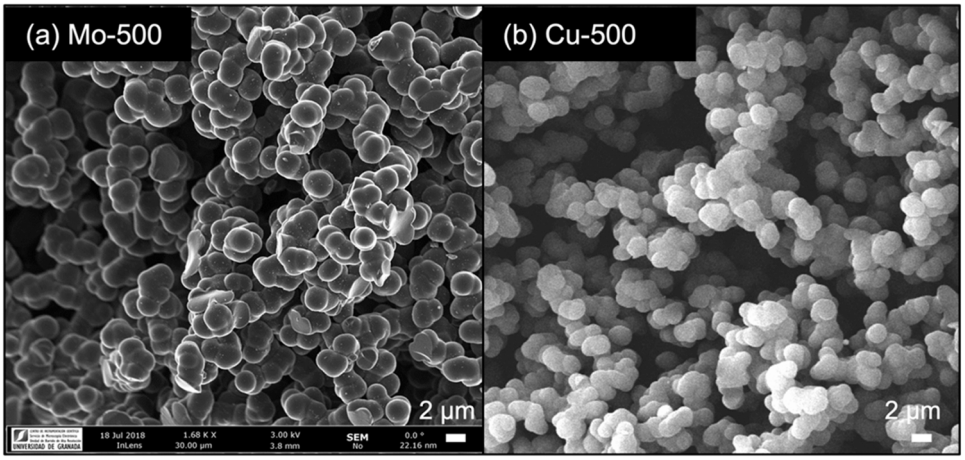

Fig. 2. Coral-like structure showing the formation of macropores between the primary particles for (a) Mo-500 and (b) Cu-500 catalysts.

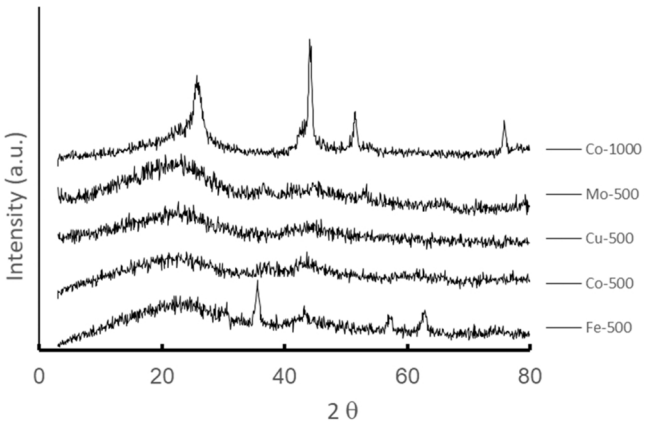

Fig. 3. XRD patterns of carbonized samples.

bonds (~288.1 eV) and COO- from carboxyl and carboxylate groups (~290.3 eV). Similarly, the O1s spectrum can be fitted with two main peaks. The component at lower BE is due mainly to M-O bonds (e. g. the Mo-O bonds are observed at ~530.7 eV) while the second peak corresponds to the oxygenated surface groups of the carbon matrix. In fact, this peak also involves two bands at BE values around ~532.0 and ~533.9 eV, corresponding to C═O and C–O bonds, respectively. The surface metal contents are in general significantly lower than the total metal content detected by TG (Table 1) thus confirming, as detected by HRTEM that some of the nanoparticles are coated by the carbon phase, becoming undetected by XPS (Table 2). The deconvoluted spectra for the different for the metallic phases are shown in Fig. S3. XPS analysis also confirms that Fe^{+3} remains unreduced [27,28] by the carbon phase during carbonization at 500 °C, as detected by XRD. A mixture of Co^{+2} and Co^{+3}, associated with peaks at binding energies (BE) of 779.4 and 785.0 eV, respectively [29] is observed for Co-500 as well, whereas in the case of Mo-doped sample, the used salt was $(NH_4)_6Mo_7O_{24}$ (Mo^{+6}) which is partially reduced to Mo^{+5}. In the case of Cu-doped samples the reduction degree is favoured, being observed M^0 species even at 500ºC, whose percentages increased with increasing the carbonization temperature up to 1000 °C, as was also detected by XRD.

3.2. Catalytic performance

TM-doped carbon aerogels were tested in the synthesis of quinoxalines from *o*-phenylenediamine **2** and benzoin **3a**, at 100 °C, using toluene as solvent, under aerobic conditions (Scheme 1). Fig. 5 depicts the catalytic performance for the synthesis of quinoxalines in the presence of the catalysts under study, notable differences between catalysts being observed. When investigating the catalysts carbonized at 500 °C, conversion values of **2** vary as follow: Mo-500 ~ Co-500 > Fe-500 > Cu-500 (Fig. 5a). Remarkably, although Mo-500 and Co-500 catalysts showed similar catalytic behavior, Mo-500 sample was found to be the most selective catalyst to the desired product **1a** (Fig. 5b). Contrarily, the Cu-500 catalyst was the least active but also totally selective giving rise to the quinoxaline **1a** (35% after 3 h) as the only reaction product. It is noteworthy that reaction rate decreases with the time in the presence of the Fe-500 aerogel.

When investigating both Fe-500 or Co-500 catalysts, the ^{1}H NMR spectra of the samples at different reaction times, beside the formation of quinoxaline **1a**, revealed the presence of the uncyclized intermediate **A** (Fe-500 = 10%; Co-500 = 5% after 3 h), previously reported when studying graphite as catalyst (Scheme 2) [30]. In addition, the presence of symmetrical signals centred at 6.5 ppm suggests the formation of hydrogenated intermediate **B** in lower conversion (2–5%) confirmed by UPLC-MS and in accordance with our previous experimental and theoretical studies [19,24].

At this regard, the formation of intermediates **A** and **B** strongly suggests that operative reaction route in the presence of Fe-500 or Co-500 catalysts probably consists of i) imination reaction, ii) imine-enamine and enol-keto tautomerizations, iii) heterocyclization, iv) dehydration and, finally, v) dehydrogenation [19,24]. Note that a non-TM doped aerogel (the RFNa sample) was also tested in the reaction resulting on 69% of conversion of **2** but notably decreased selectivity to **1a** (28%), as expected.

On the other hand, it is reasonable to think that Mo-500 and Cu-500 samples, as totally selective catalysts, could operate following a different pathway consisting of oxidation of benzoin **3a** to benzyl **4** which is able to react with **2** affording the quinoxaline **1a** (Scheme 2, pathway b). In order to explore this possibility, we also check the catalytic performance of both catalysts for the aerobic oxidation of benzoin **3a** (Scheme 2). It can be observed from Fig. 5c that Mo-500 is able to catalyse the selective oxidation of **3a** to **4** (up to 60% after 3 h) whereas Cu-500 resulted inactive in this transformation. In addition, RFNa sample was tested as reference and barely catalyzes the reaction to benzyl **4**. Considering all these results, it seems that the operative pathway strongly depends on the metallic phase doping the carbon aerogels; the Mo-500 sample probably works following the pathway b whereas Fe-500, Co-500 and Cu-500 react through pathway a.

On the other hand, differences in porosity did not influence the catalytic performance, in all cases the high porosity facilitating a good diffusion of the reagents and products. Therefore, the observed reactivity should be attributed to the type and loading of dopant metal. Considering the %M at the catalyst surface, it was observed a correlation

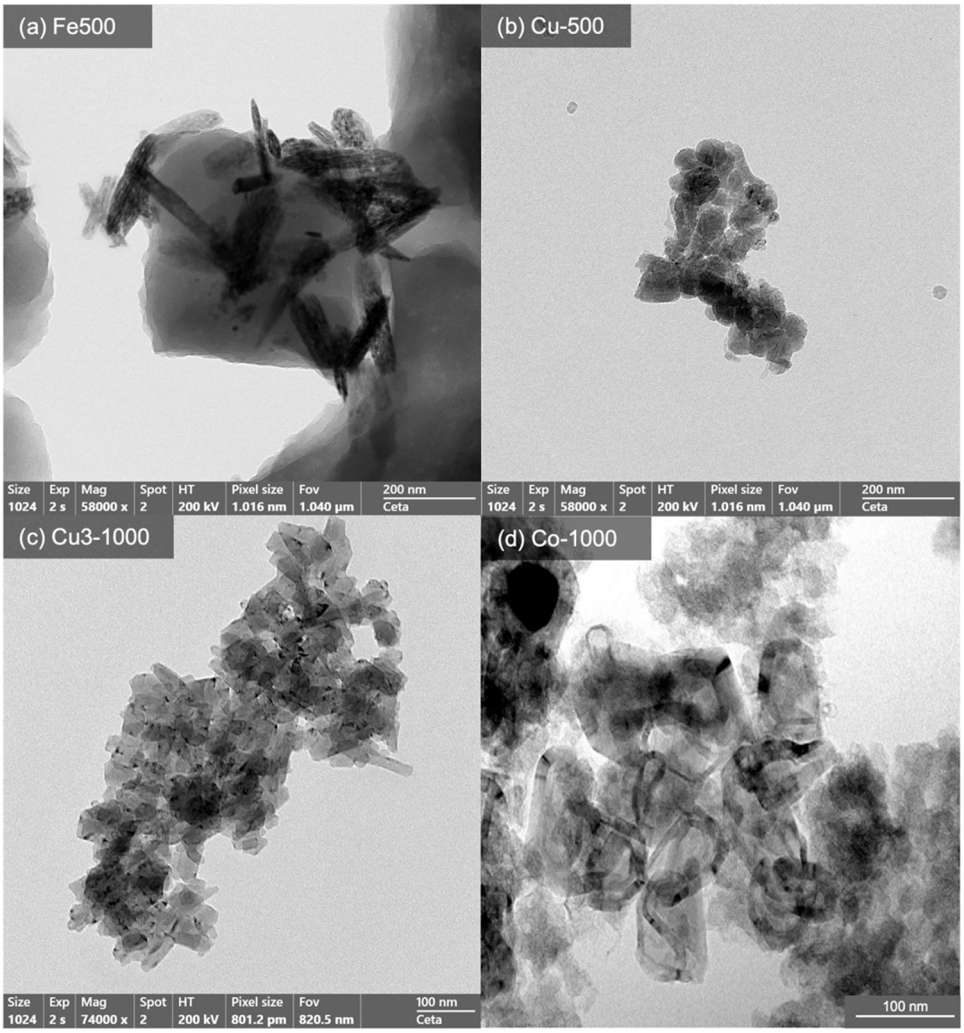

Fig. 4. TEM images of (a) Fe-500 (large Fe_2O_3 particles), (b) Cu-500 (well dispersed Cu-nanoparticles on amorphous carbon), (c) Cu3–1000 (Cu-sintering favoured by increasing loading and carbonization temperature) and (d) sintered and graphitized for Co-1000.

Table 2
Composition of the carbon surface and distribution of the metal oxidation state for the different samples determined by XPS.

Sample	C_{XPS} (%)	O_{XPS} (%)	M_{XPS} (%)	M^0 (%)/BE (eV)	M^{+n} (%)/BE (eV)
Fe-500	76.0	21.4	2.6	-	100.0 / 711.2 (Fe^{+3})
Co-500	84.8	12.0	3.2	-	68.0 / 779.4 (Co^{+2})
					32.0 / 785.0 (Co^{+3})
Cu-500	90.3	8.7	1.0	40.6 / 932.5	59.6 / 933.3 (Cu^{+2})
Cu3–1000	89.1	7.9	3.0	63.5 / 932.4	36.5 / 934.3 (Cu^{+2})
Mo-500	76.8	19.7	3.5	-	82.0/ 231.1 (Mo^{+5})
					18.0 / 233.4 (Mo^{+6})

with conversion values in such a manner that the Cu-500 sample showing the lowest metal content (1%) led to the lowest conversion to **1a** (35%, 3 h), whereas the Cu3–500 sample with increased metal loading (3%) gave the quinoxaline **1a** in higher conversion (80%, 3 h), as expected (Fig. 6a). This result is greatly interesting since investigated Cu aerogels emerged as sustainable alternative, easily prepared, more thermally stable and efficient catalysts than its homologous MOF, CuBTC [19]. Since the metal phase at the surface of TM-doped carbon aerogels is mainly composed of metal oxides, it could seem that they are the active catalytic species. However, the involvement of zero-valent metals on nanoparticles (Co and Cu catalysts) in at least some reaction step, probably in the last dehydrogenation step from intermediate **B** to compound **1a**, cannot be neglected (Scheme 2).

The influence of carbonization temperature and functionalization of the surface for TM-doped carbon catalysts in the quinoxaline synthesis were also analysed (Fig. 6). An increase of the carbonization temperature often produces an increase of the metal particle size by sintering also opening the porosity from mesopores to macropores. Concerning the catalytic behaviour of Co-1000 and Cu3–1000 samples, carbonized at 1000 °C, it was observed a diminished reaction rate in comparison with those carbonized at 500 °C, as expected; this behaviour being attributed to the bigger metal nanoparticle size but also due to the higher zero-valent metal content. In both cases quinoxaline **1a** was obtained in quantitative conversion after 3 h of reaction time.

Sample Co-1000 was also submitted to oxidant treatment with H_2O_2 leading to Co-1000PO catalyst. It is noteworthy that Co-based carbon

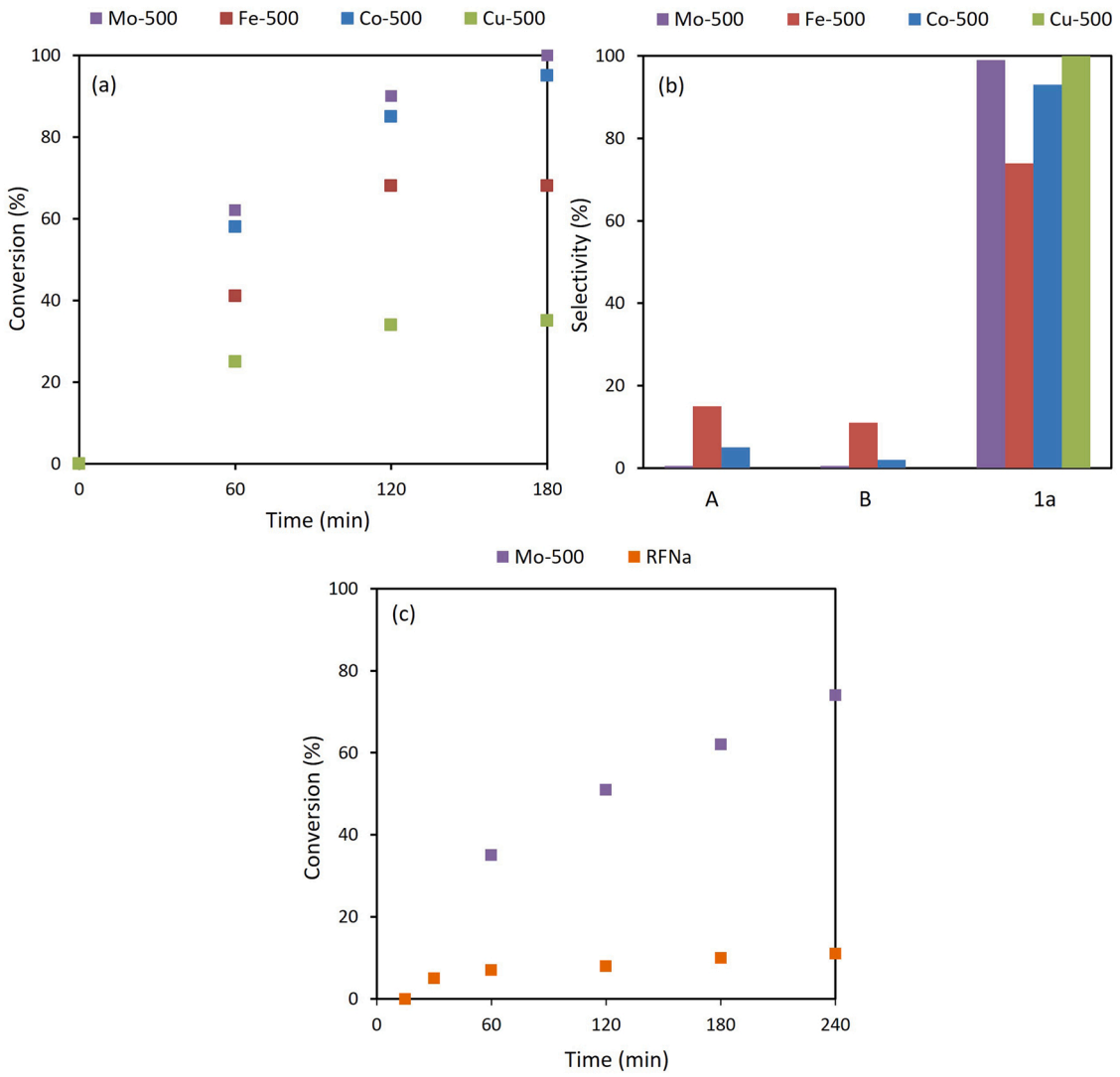

Fig. 5. (a) Conversion of **2** *vs* time and (b) selectivity values in the synthesis of quinoxaline **1a** from *o*-phenylendiamine **2** and benzoin **3a**, at 100 °C in toluene, catalyzed by carbon aerogels. (c) Aerobic oxidation of benzoin **3a**, at 100 °C, in toluene, catalyzed by carbon aerogels.

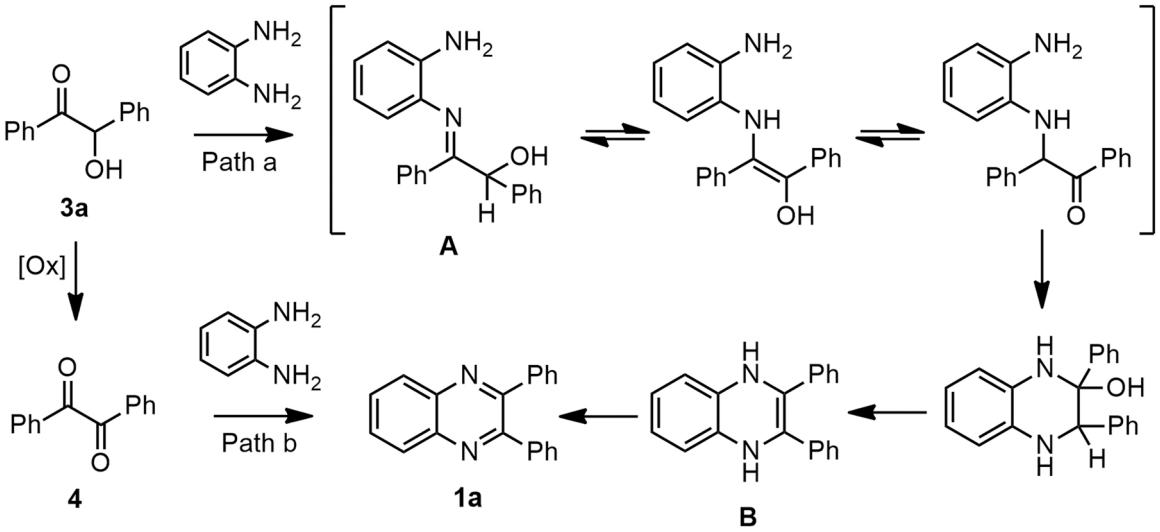

Scheme 2. Plausible pathways for the synthesis of quinoxaline **1a** from *o*-phenylenediamine **2** and benzoin **3a**.

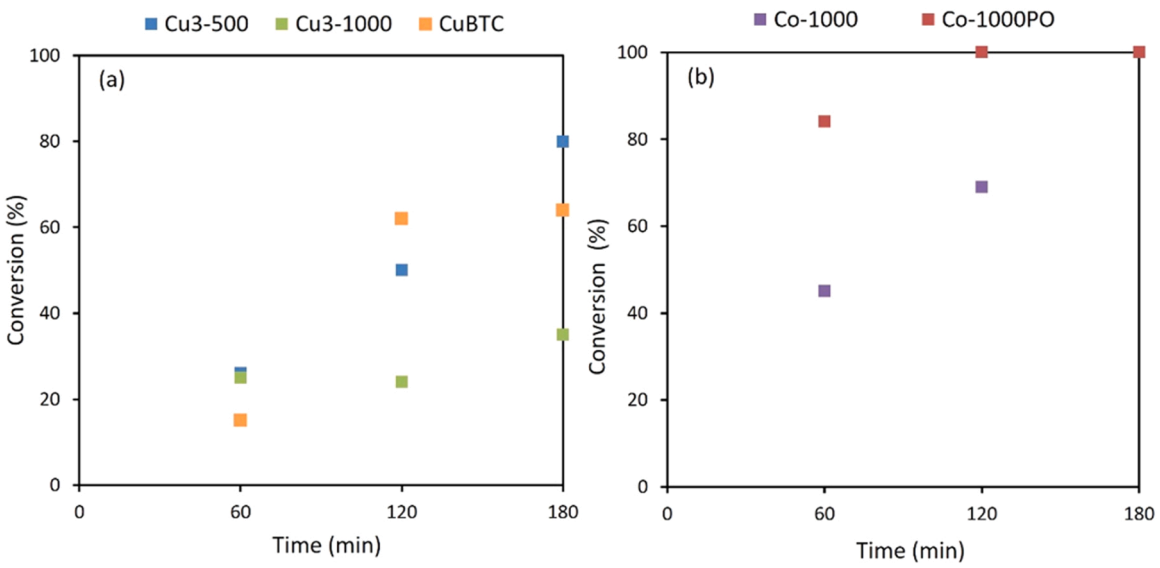

Fig. 6. Conversion of **2** *vs* time in the synthesis of quinoxaline **1a** from *o*-phenylendiamine **2** and benzoin **3a**, at 100 °C in toluene, catalyzed by carbon aerogels. Influence of (a) metal loading and carbonization temperature for Cu-doped carbon aerogels and (b) surface chemistry in Co-doped carbon aerogels.

aerogels [10] but also oxidized metal-free ones [6] were reported for the synthesis of quinolines through the Friedländer reaction, the Co-1000PO catalyst exhibiting enhanced catalytic performance as compared to the sample carbonized at 500 ºC and metal-free carbon catalysts. For this reason, this sample was selected for studying the influence of the acid surface chemistry on the catalytic performance in the synthesis of another nitrogenated heterocycle such as quinoxaline **1a**. Note that the total oxygen content of this sample determined by TPD was 3% wt; in this treatment, oxygenated surface groups (OSG) are evolved as CO_2 (300 μg/g), namely associated to the gasification of acidic groups – carboxylic, lactones, anhydrides – and CO (1275 μg/g) from OSG as phenols or carbonyl groups in ether or quinone groups. In addition, oxidation process increased the pore opening in comparison with Co-1000 precursor sample beside the creation of new oxygenated surface functions, -CO_2H among others, close the Co nanoparticles. In this case, an enhancement of the catalytic performance was observed (Fig. 6b), leading to a pure sample of quinoxaline **1a** after 3 h of reaction time, probably due to cooperative effects between Co nanoparticles and oxygenated functions. Finally, reused experiments were carried out in the presence of the most efficient catalyst, Co-1000PO sample, in the reaction of **2** and benzoin **3a**, under the same experimental conditions. However, conversion of **2** significatively decreased during the second run of the catalyst (from 99% to 69%), probably due to the interactions between nitrogen atoms in quinoxaline **1a** and acid functions from the catalyst, as expected.

In addition, the Co-1000PO sample was used for the selective catalytic synthesis of 2-phenylquinoxaline **1b** (70%), from diamine **2** and α-hydroxy acetophenone **3b**, under the same experimental conditions (Scheme 1).

Finally, information concerning carbon-based catalysts previously reported for the synthesis under study is shown in Table S1 (*see* Supporting information). It is important to note that the reaction conditions used in the synthesis of quinoxaline **1a** in some cases are different and, therefore, cannot be compared. Interestingly, TM-doped carbon catalysts herein reported are found to be sustainable alternative catalysts for the selective synthesis of quinoxalines in good-to-excellent conversions, at short reaction times, under aerobic conditions in absence of any additive. Remarkably, catalysts under study resulted more efficient and selective to quinoxaline **1a** in high conversions even as pure sample after 2 h of reaction time. In addition, some of these catalysts gave selectively the quinoxaline **1a** with increased conversion than CuBTC, a MOF wide investigated in fine chemical syntheses.

4. Conclusions

We report herein for the first time a series of carbon aerogels doped with different TMs active and selective in the synthesis of quinoxalines, from *o*-phenylenediamine **2** and α-hydroxy ketones **3**, in toluene, at 100 °C, under aerobic conditions.

Advantageously, TM-carbon gels reported herein were prepared by one-pot synthesis procedure by using pure reactants, thus obtaining free-ash pure carbon phases showing a good stability, good activity and mainly selectivity. In this case, catalytic performance is mainly governed by the presence of metal phase doping the carbon aerogel, but also conditioned by the metal loading. Metal phase at the surface of TM-doped carbon aerogels is mainly composed of the corresponding metal oxides, probably acting as predominant active catalytic sites, although the involvement of Cu^0 or Co^0 nanoparticles in the last dehydrogenation step of the reaction cannot be neglected. Enhanced reactivity observed when using Co-1000PO catalyst could be attributed to the synergistic effect between Co nanoparticles and close oxygenated functions at the surface. Remarkably, Mo-500 sample was found to be the most efficient TM-doped carbon catalyst selectively leading to the corresponding quinoxaline **1a** in high conversion. In all the cases, porosity of the samples does not seem to have any effect on the catalytic performance.

In addition, our findings provide valuable information concerning the possible reaction mechanism. While TM-doped carbon aerogels (where TM = Fe, Co, or Cu) work following the pathway a, comprising consecutive steps of i) imination, ii) imine-enamine and enol-keto tautomerizations, iii) heterocyclization, iv) dehydration and, finally, v) dehydrogenation, Mo-doped catalyst probably operates through the pathway b consisting of i) initial oxidation of benzoin **3a** to benzyl **4**, ii) double condensation reactions and iii) double dehydrations. Finally, these materials can be considered as an efficient and sustainable alternative to other catalysts recently described in our group such as acidic biomass-derived carbons but also MOF.

CRediT authorship contribution statement

Marina Godino-Ojer: Investigation, Writing – review & editing, Funding acquisition. **Sergio Morales-Torres**: Investigation, Writing – review & editing, Funding acquisition. **Francisco J. Maldonado-Hódar:** Conceptualization, Supervision, Writing – review & editing, Funding acquisition. **Elena Pérez-Mayoral:** Conceptualization, Supervision, Writing – review & editing, Funding acquisition.

Declaration of Competing Interest

The authors declare that they have no known competing financial interests or personal relationships that could have appeared to influence the work reported in this paper.

Data Availability

Data will be made available on request.

Acknowledgements

This work has been supported by Universidad Francisco de Vitoria de Madrid (Project Ref. UFV2021-21) and by the Projects ref. PID2021-126579OB-C31 and PID2021-126579OB-C32 from MCIN/AEI/10.13039/501100011033 and "ERDF A way of making Europe". S.M.-T. acknowledges to MICIN/AEI/10.13039 /501100011033 and FSE "El FSE invierte en tu futuro" for the Ramon y Cajal research contract.

Appendix A. Supporting information

Supplementary data associated with this article can be found in the online version at doi:10.1016/j.cattod.2023.01.021.

References

[1] F.J. Maldonado-Hódar, Advances in the development of nanostructured catalysts based on carbon gels, Catal. Today 218–219 (2013) 43–50, https://doi.org/10.1016/j.cattod.2013.06.005.
[2] S. Schaefer, P. Gadonneix, A. Celzard, V. Fierro, Carbon gels derived from phenolic-oil for pollutants removal in water phase, Fuel Process. Technol. 211 (2021), 106588, https://doi.org/10.1016/j.fuproc.2020.106588.
[3] J.L. Figueiredo, Carbon gels with tuned properties for catalysis and energy storage, J. Sol. -Gel Sci. Technol. 89 (2019) 12–20, https://doi.org/10.1007/s10971-018-4633-y.
[4] L.M. Pastrana-Martínez, A.M. Regadera-Macías, S. Morales-Torres, F.J. Maldonado-Hódar, Revisiting the influence of metals on resorcinol-formaldehyde carbon gels: physicochemical properties, transformations and synergism between phases, Inorg. Chim. Acta 535 (2022), 120850, https://doi.org/10.1016/j.ica.2022.120850.
[5] J. Marco-Contelles, E. Pérez-Mayoral, A. Samadi, M. do Carmo Carreiras, E. Soriano, Recent advances in the friedländer reaction, Chem. Rev. 109 (2009) 2652–2671, https://doi.org/10.1021/cr800482c.
[6] M. Godino-Ojer, E. Soriano, V. Calvino-Casilda, F.J. Maldonado-Hódar, E. Pérez Mayoral, Metal-free synthesis of quinolines catalyzed by carbon aerogels: influence of the porous texture and surface chemistry, Chem. Eng. J. 314 (2017) 488–497, https://doi.org/10.1016/j.cej.2016.12.006.
[7] Bailón-García, F. Carrasco-Marín, A.F. Pérez-Cadenas, F.J. Maldonado-Hódar, Selective hydrogenation of citral by noble metals supported on carbon xerogels: catalytic performance and stability, Appl. Catal. A 512 (2016) 63–73, https://doi.org/10.1016/j.apcata.2015.12.017.
[8] K. Kreek, K. Kriis, B. Maaten, M. Uibu, A. Mere, T. Kanger, M. Koel, Organic andcarbon aerogels containing rare-earth metals: their properties and application as catalysts, J. Non-Cryst. Sol. 404 (2014) 43–48, https://doi.org/10.1016/j.jnoncrysol.2014.07.021.
[9] E. Pérez-Mayoral, M. Godino-Ojer, A.J. López Peinado, F.J. Maldonado-Hódar, Highly efficient and selective catalytic synthesis of quinolines involving transition metals-doped carbon aerogels, ChemCatChem 9 (2017) 1422–1428, https://doi.org/10.1002/cctc.201601657.
[10] M. Godino-Ojer, R.M. Martín-Aranda, F.J. Maldonado-Hódar, A.F. Pérez-Cadenas, E. Pérez-Mayoral, Developing strategies for the preparation of Co-carbon catalysts involved in the free solvent selective synthesis of aza-heterocycles, Mol. Catal. 445 (2018) 223–231, https://doi.org/10.1016/j.mcat.2017.11.037.
[11] M. Godino-Ojer, A.J. López-Peinado, F.J. Maldonado-Hódar, E. Bailón-García, E. Pérez-Mayoral, Cobalt oxide–carbon nanocatalysts with highly enhanced catalytic performance for the green synthesis of nitrogen heterocycles through the Friedländer condensation, Dalton Trans. 48 (2019) 5637–5648, https://doi.org/10.1039/C8DT04403A.
[12] M. Godino-Ojer, S. Morales-Torres, E. Pérez-Mayoral, F.J. Maldonado-Hódar, Enhanced catalytic performance of ZnO/carbon materials in the green synthesis of poly-substituted quinolines, J. Environ. Chem. Eng. 10 (2022), 106879, https://doi.org/10.1016/j.jece.2021.106879.
[13] V.K. Maikhuri, A.K. Prasad, A. Jha, S. Srivastava, Recent advances in the transition metal catalyzed synthesis of quinoxalines: a review, N. J. Chem. 45 (2021) 13214–13246, https://doi.org/10.1039/D1NJ01442K.
[14] S. Sithambaram, Y. Ding, W. Li, X. Shen, F. Gaenzler, S.L. Sui, Manganese octahedral molecular sieves catalyzed tandem process for synthesis of quinoxalines, Green. Chem. 10 (2008) 1029–1032, https://doi.org/10.1039/B805155K.
[15] K.T. Venkateswara Rao, P.S. Sai Prasad, N. Lingaiah, Iron exchanged molybdophosphoric acid as an efficient heterogeneous catalyst for the synthesis of quinoxalines, J. Mol. Catal. A Chem. 312 (2009) 65–69, https://doi.org/10.1016/j.molcata.2009.07.005.
[16] C.S. Cho, W.X. Ren, A recyclable copper catalysis in quinoxaline synthesis from α-hydroxyketones and o-phenylenediamines, J. Organomet. Chem. 694 (2009) 3215–3217, https://doi.org/10.1016/j.jorganchem.2009.06.002.
[17] A. Kamal, K.S. Babu, S.M. Ali Hussaini, R. Mahesh, A. Alarifi, Amberlite IR-120H, an efficient and recyclable solid phase catalyst for the synthesis of quinoxalines: a greener approach, Tetrahedron Lett. 56 (2015) 2803–2808, https://doi.org/10.1016/j.tetlet.2015.04.046.
[18] G.H. Dang, Y.T.H. Vu, Q.A. Dong, D.T. Le, T. Truong, N.T.S. Phan, Quinoxaline synthesis via oxidative cyclization reaction using metal–organic framework Cu (BDC) as an efficient heterogeneous catalyst, Appl. Catal. A Gen. 491 (2015) 189–195, https://doi.org/10.1016/j.apcata.2014.11.009.
[19] M. Godino-Ojer, M. Shamzhy, J. Čejka, E. Pérez-Mayoral, Basolites: a type of metal organic frameworks highly efficient in the onepot synthesis of quinoxalines from α-hydroxy ketones under aerobic conditions, Catal. Today 345 (2020) 258–266, https://doi.org/10.1016/j.cattod.2019.08.002.
[20] A.V. Kumar, V.P. Reddy, K.R. Rao, Aqueous-Phase aerobic oxidation of alcohols by Ru/C in the presence of cyclodextrin: one-pot biomimetic approach to quinoxaline synthesis, Synlett 17 (2010) 2571–2574, https://doi.org/10.1055/s-0030-1258775.
[21] N. Shah, E. Gravel, D.V. Jawale, E. Doris, I.N.N. Namboothiri, Synthesis of quinoxalines by a carbon nanotube–gold nanohybrid-catalyzed cascade reaction of vicinal diols and keto alcohols with diamines, ChemCatChem 7 (2015) 57–61, https://doi.org/10.1002/cctc.201402782.
[22] D. Panja, B. Paul, B. Balasubramaniam, R.K. Gupta, S. Kundu, Application of a reusable Co-based nanocatalyst in alcohol dehydrogenative coupling strategy: synthesis of quinoxaline and imine scaffolds, Catal. Commun. 137 (2020), 105927, https://doi.org/10.1016/j.catcom.2020.105927.
[23] K. Sun, D. Li, G.-P. Lu, C. Cai, Hydrogen auto-transfer synthesis of quinoxalines from o-Nitroanilines and biomass-based diols catalyzed by MOF-derived N,P codoped cobalt catalysts, ChemCatChem 13 (2021) 373–381, https://doi.org/10.1002/cctc.202001362.
[24] M. Godino-Ojer, R. Blazquez-García, I. Matos, M. Bernardo, I.M. Fonseca, E. Pérez Mayoral, Porous carbons-derived from vegetal biomass in the synthesis of quinoxalines. Mechanistic insights, Catal. Today 354 (2020) 90–99, https://doi.org/10.1016/j.cattod.2019.06.043.
[25] V. Jeena, Ross S. Robinson, Green oxidations: titanium dioxide induced tandem oxidation coupling reactions, Beilstein J. Org. Chem. 5 (2009) 1–4, https://doi.org/10.3762/bjoc.5.24.
[26] C. Lin, J.A. Ritter, Effect of synthesis pH on the structure of carbon xerogels, Carbon 35 (1997) 1271–1278, https://doi.org/10.1016/S0008-6223(97)00069-9.
[27] C. Moreno-Castilla, F.J. Maldonado-Hodar, A.F. Perez-Cadenas, Physicochemical surface properties of Fe, Co, Ni, and Cu-Doped monolithic organic aerogels, Langmuir 19 (2003) 5650–5655, https://doi.org/10.1021/la034536k.
[28] B.M. Esteves, S. Morales-Torres, F.J. Maldonado-Hodar, L.M. Madeira, Sustainable iron-olive stone-based catalysts for Fenton-like olive mill wastewater treatment: development and performance assessment in continuous fixed-bed reactor operation, Chem. Eng. J. 435 (2022), 134809, https://doi.org/10.1016/j.cej.2022.134809.
[29] F. Akti, Green synthesis of pistachio shell-derived biochar supported cobalt catalysts and their catalytic performance in sodium borohydride hydrolysis, Int. J. Hydroge Energy 47 (2022) 35195–35202, https://doi.org/10.1016/j.ijhydene.2022.08.101. ⟨https://srdata.nist.gov/xps/⟩.
[30] H.K. Kadam, S. Khan, R.A. Kunkalkar, S.G. Tilve, Graphite catalyzed green synthesis of quinoxalines, Tetrahedron Lett. 54 (2013) 1003–1007, https://doi.org/10.1016/j.tetlet.2012.12.041.